Computational and Structural Biotechnology Journal 20 (2022) 1876–1884

COMPUTATIONAL AND STRUCTURAL BIOTECHNOLOGY JOURNAL

journal homepage: www.elsevier.com/locate/csbj

Investigation of potential descriptors of chemical compounds on prevention of nephrotoxicity via QSAR approach

Hung-Jin Huang [a], Yu-Hsuan Lee [b], Chu-Lin Chou [a,c,d,e], Cai-Mei Zheng [a,c,d,*], Hui-Wen Chiu [d,f,g,*]

[a] Division of Nephrology, Department of Internal Medicine, School of Medicine, College of Medicine, Taipei Medical University, Taipei, Taiwan
[b] Department of Cosmeceutics, China Medical University, Taichung, Taiwan
[c] Division of Nephrology, Department of Internal Medicine, Shuang Ho Hospital, Taipei Medical University, Taiwan
[d] TMU Research Center of Urology and Kidney, Taipei Medical University, Taipei, Taiwan
[e] Division of Nephrology, Department of Internal Medicine, Hsin Kuo Min Hospital, Taipei Medical University, Taoyuan City, Taiwan
[f] Graduate Institute of Clinical Medicine, College of Medicine, Taipei Medical University, Taipei, Taiwan
[g] Department of Medical Research, Shuang Ho Hospital, Taipei Medical University, New Taipei City, Taiwan

ARTICLE INFO

Article history:
Received 28 January 2022
Received in revised form 2 April 2022
Accepted 11 April 2022
Available online 15 April 2022

Keywords:
Nephrotoxicity
QSAR
Genetic algorithm

ABSTRACT

Drug-induced nephrotoxicity remains a common problem after exposure to medications and diagnostic agents, which may be heightened in the kidney microenvironment and deteriorate kidney function. In this study, the toxic effects of fourteen marked drugs with the individual chemical structure were evaluated in kidney cells. The quantitative structure–activity relationship (QSAR) approach was employed to investigate the potential structural descriptors of each drug-related to their toxic effects. The most reasonable equation of the QSAR model displayed that the estimated regression coefficients such as the number of ring assemblies, three-membered rings, and six-membered rings were strongly related to toxic effects on renal cells. Meanwhile, the chemical properties of the tested compounds including carbon atoms, bridge bonds, H-bond donors, negative atoms, and rotatable bonds were favored properties and promote the toxic effects on renal cells. Particularly, more numbers of rotatable bonds were positively correlated with strong toxic effects that displayed on the most toxic compound. The useful information discovered from our regression QSAR models may help to identify potential hazardous moiety to avoid nephrotoxicity in renal preventive medicine.

1. Introduction

Toxic nephropathy is an important topic and relatively general term of kidney damage to cause acute and chronic renal failure by toxic effects of chemicals [1], and the mechanisms of nephrotoxicity include inflammation, tubular cell toxicity, and crystal nephropathy [2]. Nephrotoxicity is frequently induced by a wide spectrum of therapeutic drugs and environmental pollutants [3]. The nephrotoxicity of kidney disease can be classified into two types: Acute kidney injury (AKI) and chronic kidney disease (CKD) [4]. The AKI is characterized by rapid impairment of kidney function and is defined as an increase in serum creatinine concentration and duration $\leq$ 7 days, leading to an acute decreased glomerular filtration rate (GFR) [5]. Clinically, untreated AKI will lead to CKD and quickly develop to end-stage renal disease (ESRD) in most cases. The CKD is defined as abnormal kidney function or glomerular filtration rate (GFR) less than 60 mL/min/1.73 m^2, albuminuria > 30 mg/24 h, and presence of kidney damage marker for three months [6]. In other cases, the progression of CKD to ESRD is closely related to the accumulation of toxic metabolites in the patient's blood [7]. The underlying condition such as renal fibrosis, kidney tubular damage, vascular insufficiency, glomerular hypertension, and vascular endothelial cell damage may cause the AKI

Abbreviations: AKI, acute kidney injury; CKD, chronic kidney disease; GFR, glomerular filtration rate; ESRD, end-stage renal disease; DIKD, drug-induced kidney disease; QSAR, quantitative structure-activity relationship; KCSF, keratinocyte serum-free; SRB, sulforhodamine B; PBS, phosphate buffered saline; GFA, genetic function approximation.

* Corresponding authors at: Division of Nephrology, Department of Internal Medicine, School of Medicine, College of Medicine, Taipei Medical University, 250 Wu-Hsing Street, Taipei 110, Taiwan (C.-M. Zheng). Graduate Institute of Clinical Medicine, College of Medicine, Taipei Medical University, 250 Wu-Hsing Street, Taipei 110, Taiwan (H.W. Chiu).

E-mail addresses: 11044@s.tmu.edu.tw (C.-M. Zheng), leu3@tmu.edu.tw (H.-W. Chiu).

https://doi.org/10.1016/j.csbj.2022.04.013

progression into CKD [8]. Therefore, both AKI and CKD are unifying and can be considered as risk factors for each other.

Recent reports have indicated that drug-induced nephrotoxicity may cause by cumulative dose-dependent toxicity and is recognized as a contributor to kidney injury resulting in AKI and CKD [9]. Clinically, numerous drugs are used to treat multiple diseases that have the nephrotoxic impact on the nephron directly [10], the common problems include renal dysfunction [11], fluid-electrolyte disorders [12], and sepsis [13] after exposure to nephrotoxic drugs during therapy. The nephrotoxic drugs can cause damage to tubules and nephrons by entering proximal tubular cells through cellular uptake or apical drug transport [14]. Drug-induced kidney disease (DIKD) is an origin of kidney disease that constitutes a major cause of AKI and CKD in current clinical practice [15]. Several prospective studies of AKI have demonstrated that approximately 14–26% of critically ill patients with AKI diagnoses were treated with nephrotoxic drugs [16,17]. Therefore, the prevention of drug-related nephrotoxicity before starting the treatment is an important issue to avoid or diminish renal toxicity. Herein, we focused on toxicity assessment to investigate the chemical information about toxic substances that cause adverse effects on kidney cells.

In consideration of unethical animal procedures, alternatives to animal testing could be used to avoid the drawbacks of animal experiments [18]. According to the 3Rs principle published by Russell and Burch, the efforts to reduce, refine and replace animal tests were developed in recent years to perform more humane animal research [19]. In order to reduce the number of experimental animals, various alternative methods of experimental animals have been suggested including computer-based models [20], cells and tissue cultures [21], invertebrates [22], alternative organisms [23], and microorganisms [24]. The aforementioned methods provide good strategies to overcome the major concern of ethics. Besides, the advantages associated with the alternative methods in the assessment of hazardous chemicals are cost-effectiveness, time efficiency, and less ethical concern [25]. In some cases, combining in silico and in vitro approaches have the potential to estimate the likelihood of hazardous compounds statistically [26–28]. Therefore, we focused on the relationship between the toxin structures and their nephrotoxicity in this study. The quantitative structure–activity relationship (QSAR) is one of the computer-based drug design methods employed in pharmaceutical sciences and lead optimization [29], which is also called indirect drug designing in the field of computational modeling [30]. The QSAR can provide predictive models based on mathematical methods that can be employed to study the design of known types of chemical compounds to reach an improved activity [31]. In general, the QSAR techniques were regarded as a cost-effective tool in precaution of the toxicants for human health and environmental safety [32,33]. However, there are still very few studies focused on the nephrotoxic using in silico model such as QSAR modeling in predicting human nephrotoxicity for drug development [34]. To identify for investigation of therapeutic drugs with non-nephrotoxic, we aim to investigate the relationship between chemical structure and its nephrotoxicity.

Here, we explored the potential of developing predictive QSAR models for a series of toxic chemicals acting as inhibitors of renal cells. A series of fourteen different compounds were evaluated for the activity on the HK-2 cell line. Meanwhile, identification of the potential chemical addends on the chemicals was investigated using QSAR models. The QSAR models were constructed with the GA algorithm to construct the relationship between structural changes and nephrotoxicity, which can be applied to predict the nephrotoxicity for new chemical compounds and provide a new guideline for the development of non-nephrotoxic drugs. The information from the experimental data and equations of predictive computer models might guide the potential functional groups on chemicals that are related to toxic nephropathies of kidney cells.

2. Materials and methods

2.1. Cell cultures and test compounds

The human kidney proximal tubular epithelial cell line HK-2 was purchased from American Type Culture Collection (CRL2190). Cells were cultured keratinocyte serum-free (KCSF) medium containing bovine pituitary extract (40 μg/mL) and recombinant epidermal growth factor (5 ng/mL) (Gibco BRL, Grand Island, NY, USA). The cultured cells were maintained in a humidified 5% CO_2 chamber at 37℃. The cultured medium replacement was performed two times every week. A density around 1×10^5 for HK-2 cell lines was respectively seeded in each well of 96-well plates then maintained in the humidified incubator for 24 h before treatment with test compounds. All dissolve solutions of Thapsigargin, 4-Deoxy Nivalenol, Ochratoxin A, Ochratoxin B, Fusarenon X, 15-O-Acetyl-4-deoxynivalenol, Cinacalcet, Tacrolimus, Mitomycin C, Pantoprazole (Cayman Chemical, Ann Arbor, MI, USA), Aristolochic acid I (Sigma-Aldrich Corp., St. Louis, MO, USA), Cisplatin, Amphotericin B, and Cyclosporine A (MedChemExpress, Monmouth Junction, NJ, USA) were prepared before cell viability assay.

2.2. Cell viability assay

Sulforhodamine B (SRB) assay was used to evaluate the biological activity of HK-2 for test compounds. After 24 h incubation time with each test compound in 96-well plates, cells were washed with Phosphate buffered saline (PBS) solution two times and then fixed with a trichloroacetic acid solution for 1 h. The supernatant was removed, and each well was washed two times before SRB staining (Sigma-Aldrich Corp.) After 1 h staining, the residual dye was removed and then washed two times with 1% acetic acid. Subsequently, Tris-buffer (20 mM) was added to each well and then the absorbance of the colored solution was measured at a test wavelength of 562 nm via an absorbance microplate reader (Molecular Devices, Sunnyvale, CA, USA).

The percentage of cell viability was calculated according to the following equation:

$$\text{Cell viability}\,\% = \frac{AbsSample - AbeBlank}{AbsControl - AbsBlank} \times 100\% \quad (1)$$

where AbsSample indicates the optical density of cells with tested compounds, AbsControl means the optical density of control cells, and AbsBlank is the absorbance of PBS.

2.3. Construction of QSAR models

A set of 14 compounds with measured bioactivity data (IC_{50} values) were utilized for the QSAR model generation. The 2D structure of each molecule was created using BIOVIA Discovery Studio (BIOVIA, USA), and the molecular properties of the compounds were calculated with the Calculate Molecular Properties module of Discovery Studio software. Before the process of the QSAR model study, all of the IC_{50} values (in μM) were converted to pIC_{50} values using eq 2:

$$pIC_{50} = -\log IC_{50} \times 10^6 \quad (2)$$

The genetic function approximation (GFA) algorithm was used to generate equations of the QSAR model, which contains molecular descriptors correlating with the activity values. The GFA algo-

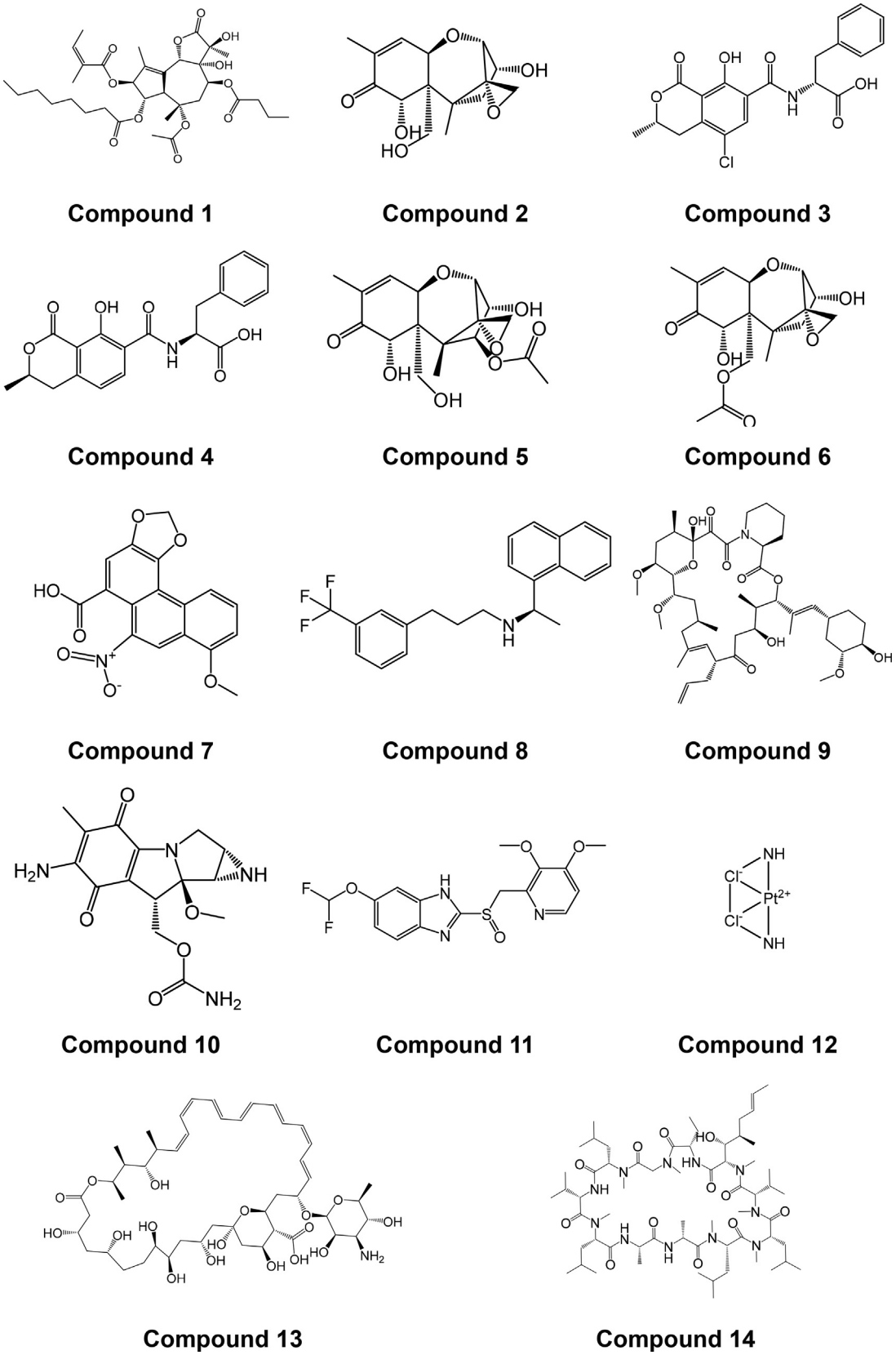

Fig. 1. The chemical structure of compounds **1**–**14** used in cell viability assay on HK-2 cells.

rithm was employed to select suitable properties related to the activity value. The detailed settings of QSAR model generation were displayed in Table S1.

2.4. Statistical analysis

The experimental data were displayed as the means ± standard deviation (SD), and the differences between each group were measured by one-way analysis of variance. Each experimental data was performed independently three times for reproducibility. The value of cross-validation (q^2) to evaluate the accuracy of each QSAR model was measured by the following equation:

$$q^2 = 1 - \frac{PRESS}{TSS} \quad (3)$$

where PRESS indicated the predicted residual error sum of squares, and the TSS means the total sum of squares of the differences.

3. Results

3.1. Cell viability

The molecular structures of fourteen chemical compounds used to determine the biological inhibitory effects for HK-2 cells are shown in Fig. 1. The standard deviation (SD) of each measured half-lethal inhibition concentration (IC_{50}) value was estimated from three independent experimental groups via SRB assay. The calculated IC_{50} values for HK-2 cells treated with the aforementioned fourteen compounds are listed in Table 1. After treatment with the fourteen chemical compounds for 24 h, the cell viability of HK-2 cells decreased in a dose-dependent. Compounds **1** and **5** displayed significant cytotoxicity on HK-2 cells, which have IC_{50} values of 0.18 μM and 0.35 μM, respectively (Fig. 2). Compounds **6**, **10**, and **13** are more effective than the other compounds, and their IC_{50} values have unit digits for HK-2 cells (Fig. 3). Compounds **2**, **3**, **4**, **8**, **9**, **10**, **12**, and **14** have slightly inhibitory effects among the tested chemical compounds, and the estimated bioactivity value has micromolar of tens digit. However, the IC_{50} value of compound **11** is 299.6 μM due to low toxicity (Fig. 3).

3.2. QSAR modeling

The measured IC_{50} values of HK-2 cells were regarded as the activity to generate three different simple linear regression models for the fourteen chemical compounds. The molecular descriptors were generated from the QSAR analyzing tools of BIOVIA Discovery Studio. The potent molecular descriptors of the aforementioned chemicals related to pIC_{50} values were identified via the GFA algorithm. The chemical structures and the measured IC_{50} values used for the model generation are listed in Table 2. The equation of the suggested QSAR model is described as follows:

$$\begin{aligned} \text{Predicted } IC_{50} = {} & -3.0506 - 0.1228 \times \text{CCount} + 0.014105 \\ & \times \text{NumBridgeBonds} + 0.94643 \times \text{NumHDonors} \\ & + 0.15129 \times \text{NumNegativeAtoms} - 2.7209 \\ & \times \text{NumRingAssemblies} + 2.7209 \times \text{NumRings3} \\ & + 2.9782 \times \text{NumRings6} + 0.87064 \times \text{NumRotatableBonds} \end{aligned} \quad (4)$$

The least-squares fitting R^2, adjusted R^2, and cross-validated correlation coefficient q^2 values were three criteria for QSAR model validation. The top 1 equation of the QSAR model, which had R^2 of 0.9988, adj R^2 of 0.9968, and q^2 of 0.9582, were defined as a reasonable model due to the best match between the predicted and experimental activity as displayed in Fig. 4. In order to evaluate the effectiveness of QSAR models constructed by the data set of all test compounds, the top ten QSAR models with acceptable statistics for both training and test sets were displayed in Table S2. To develop an external validation of QSAR models, the dataset was randomly split into training (70% = 10 chemicals) and external (30% = 4 chemicals) subsets [35,36]. The best reasonable QSAR model contained training and test compounds are plotted in Figure S1.

The value of cross-validation q^2 beyond 0.6 indicated the individual generated equations of the HK-2 cells with accuracy. The residual errors between the predicted and observed values of all chemical compounds were summarized in Table 3. The data showed that each value of the residual error was below 0.1, which illustrated the recommended QSAR model with high predicted power.

3.3. Quantitative descriptors of the QSAR equation

As for the best reasonable equation of the toxicity for HK-2 cells, the molecular descriptors of the fourteen chemical compounds relative to bioactivities of HK-2 cells include **C_Count**, **Num_BridgeBonds**, **Num_H_Donors**, **Num_NegativeAtoms**, **Num_RingAssemblies**, **Num_Rings3**, **Num_Rings6**, and **Num_RotatableBonds**. In order to investigate relation, the quantitative data of the aforementioned descriptors for the fourteen chemical compounds are computed and displayed in Table 4. Here, **C_Count** means the number of carbon atoms in the structure of a chemical compound. **Num_BridgeBonds** indicates bonds in a bridgehead ring system and is defined as how many rings share one bond in common. **Num_H_Donors** is the number of hydrogen bond donors including heteroatoms (Oxygen, Nitrogen, Sulfur, or Phosphorus) to form hydrogen bonds. **Num_NegativeAtoms** means the number of atoms with a negative charge. **Num_RingAssemblies** is defined as the number of fragments remaining when all non-ring bonds are removed from a chemical structure. For instance, the two ring assemblies indicate two benzene rings joined directly by single bonds, while one ring assembly has one or without benzene rings. **Num_Rings3** is defined as the number of three-membered rings in one organic compound. **Num_Rings6** indicates the number of six-membered rings among the structure of a chemical compound. As for the last descriptor,

Table 1
The biological activity of HK-2 cells after exposure to various chemicals for 24 h. The cell viability was measured by SRB assay.

Comp.	Name	CAS	IC_{50} (μM)
1	Thapsigargin	67526–95-8	0.18
2	4-Deoxy Nivalenol	51481–10-8	12.31
3	Ochratoxin A	303–47-9	46.15
4	Ochratoxin B	4825–86-9	37.86
5	Fusarenon X	23255–69-8	0.35
6	15-O-Acetyl-4-deoxynivalenol	88337–96-6	3.77
7	Aristolochic acid I	313–67-7	102.60
8	Cinacalcet	226256–56-0	17.14
9	Tacrolimus	104987–11-3	49.39
10	Mitomycin C	50–07-7	5.04
11	Pantoprazole	102625–70-7	299.60
12	Cisplatin	15663–27-1	25.45
13	Amphotericin B	1397–89-3	3.70
14	Cyclosporine A	59865–13-3	38.27

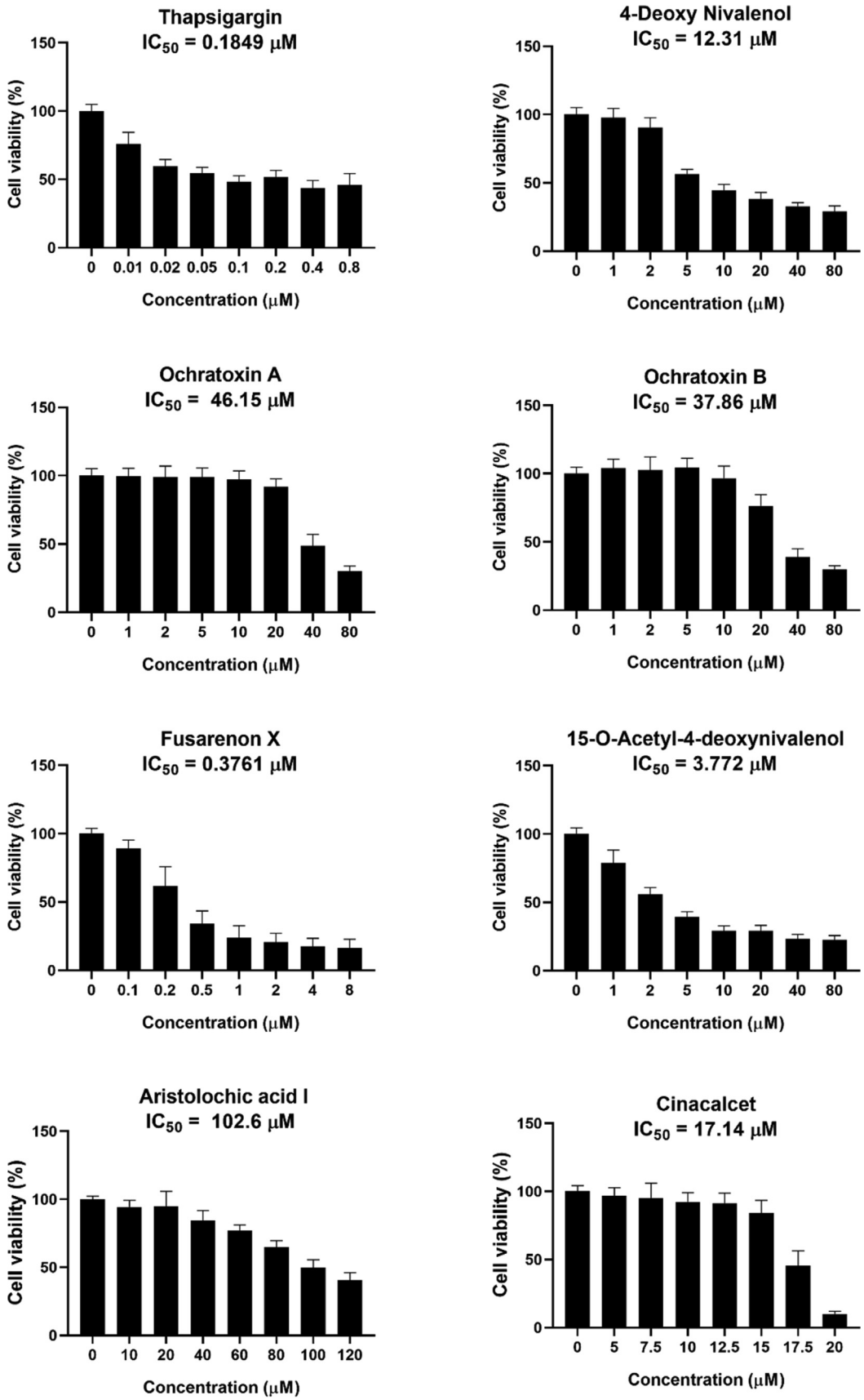

Fig. 2. The effects of compounds **1**–**8** on the viability of HK-2 cells after treatment with compounds in dose-dependent manner measured by the SRB assay for 24 h. Data of cell viability were shown as the mean ± SD of three independent experiments. Cell viability % = [(mean optical density of the sample − blank)/ (mean optical density of the control − blank)] × 100%.

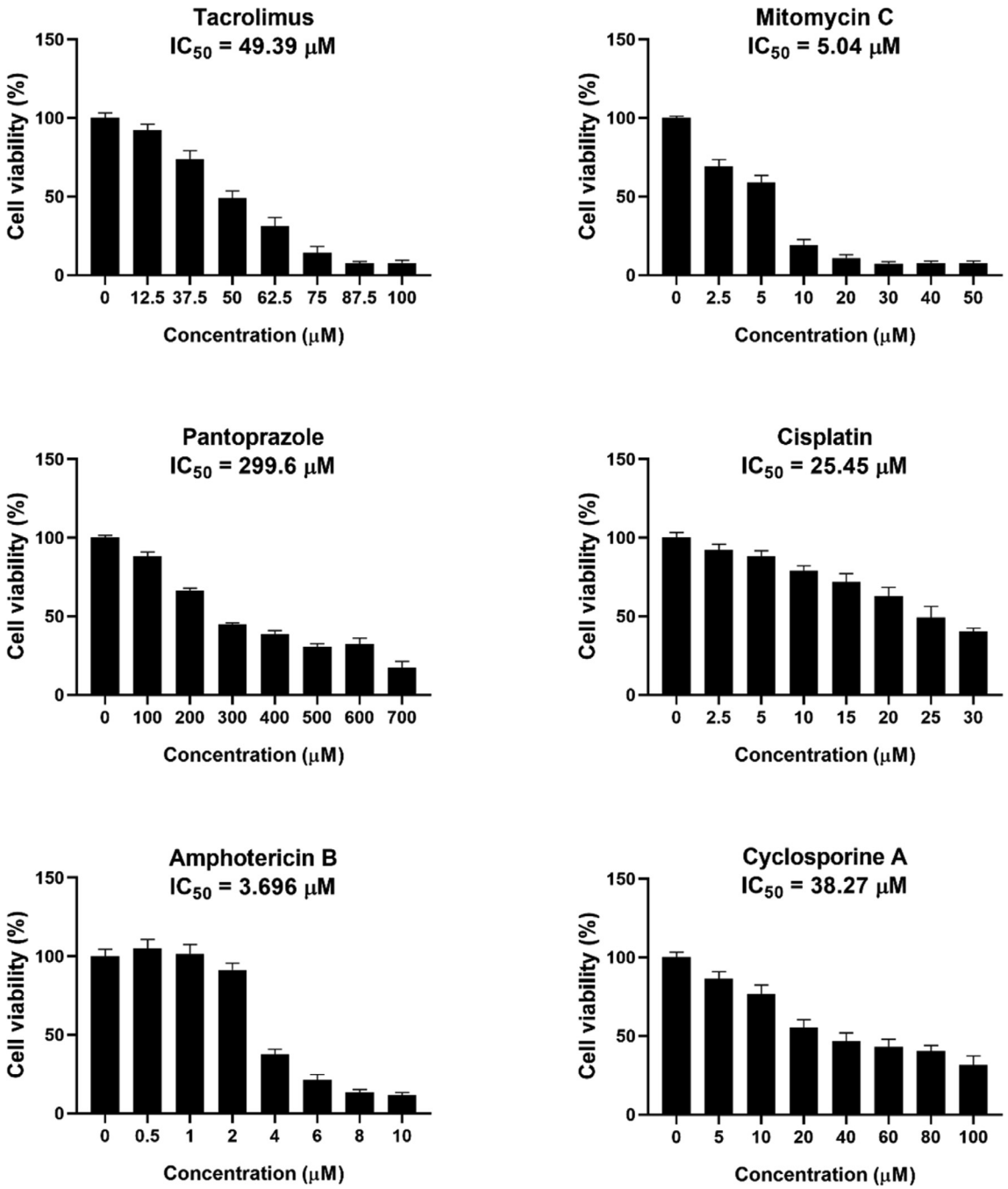

Fig. 3. The effects of compounds **9**–**14** on the viability of HK-2 cells after treatment with compound measured by the SRB assay for 24 h.

Num_RotatableBonds is the number of single bonds between heavy atoms that are attached to only hydrogens.

4. Discussion

Animal ethics and animal consciousness has been considered an important issue in recent years [37]. To avoid unethical procedures, in vitro cell-based methods and in silico approaches are useful strategies of alternatives to minimize the experimental animals used in the assessment of kidney toxicity to reduce costs and time. The QSAR method can provide a useful strategy to identify key features based on the relationship between the Physico-chemical properties of each chemical and their biological activities for the investigation of nephrotoxic. The GA algorithm applied in QSAR studies can generate interpretable equations with numerical estimation to link molecular descriptors to the biological activity, which has been applied in various areas of drug design such as leading drug optimization [38] and predictive toxicology [39].

In comparison with early reports, 3D-QSAR and 4D-QSAR approaches were regarded as useful strategies to construct pharmacophore features, and the most frequently used methods include Comparative Molecular Field Analysis (CoMFA), Comparative Molecular Similarity Indices Analysis (CoMSIA) and GRID/GOLPE program. The regression of the 3D-QSAR approach was applied using a partial least squares (PLS) algorithm to establish the optimal number of descriptors in structure-based pharmacophore modeling under PHASE software [40,41]. To build the 4D-QSAR model, the electron-conformational genetic algorithm

Table 2
Top ten QSAR models generated by genetic function approximation (GFA) algorithm for HK-2 cells and ranked by values of correlation coefficient (r^2).

Index	QSAR models	r^2	r^2 (adj)	q^2	p-value
1.	GFATempModel_1 = 3.0506–0.1228 * C_Count + 0.014105 * Num_BridgeBonds + 0.94643 * Num_H_Donors + 0.15129 * Num_NegativeAtoms – 2.7209 * Num_RingAssemblies + 2.7209 * Num_Rings3 + 2.9782 * Num_Rings6 + 0.87064 * Num_RotatableBonds	0.9988	0.9968	0.9582	7.61E-07
2.	GFATempModel_2 = -3.2614–0.12267 * C_Count + 0.14995 * Num_BridgeHeadAtoms + 0.9651 * Num_H_Donors + 0.22799 * Num_NegativeAtoms – 2.5999 * Num_RingAssemblies + 2.6853 * Num_Rings3 + 2.9419 * Num_Rings6 + 0.87257 * Num_RotatableBonds	0.9982	0.9954	0.8957	1.85E-06
3.	GFATempModel_3 = -2.6452–0.10623 * C_Count – 0.045306 * N_Count + 0.92158 * Num_H_Donors + 0.11012 * Num_NegativeAtoms – 2.5817 * Num_RingAssemblies + 2.6126 * Num_Rings3 + 2.799 * Num_Rings6 + 0.8085 * Num_RotatableBonds	0.9977	0.9941	0.8721	3.56E-06
4.	GFATempModel_4 = -3.9427–0.05922 * H_Count – 0.20301 * IsChiral + 0.14684 * Num_BridgeHeadAtoms + 0.9517 * Num_H_Donors – 2.5379 * Num_RingAssemblies + 3.0888 * Num_Rings3 + 2.828 * Num_Rings6 + 0.84963 * Num_RotatableBonds	0.9977	0.9939	0.9703	3.78E-06
5.	GFATempModel_5 = -1.7591–0.14381 * C_Count + 0.97518 * Num_H_Donors – 2.9476 * Num_RingAssemblies + 0.72947 * Num_Rings + 1.7158 * Num_Rings3 – 0.94125 * Num_Rings5 + 2.2146 * Num_Rings6 + 0.82905 * Num_RotatableBonds	0.9976	0.9938	0.8242	3.93E-06
6.	GFATempModel_6 = -4.2701–0.12096 * C_Count + 0.06777 * O_Count + 0.032085 * Num_AromaticBonds + 0.97449 * Num_H_Donors – 2.6918 * Num_RingAssemblies + 3.195 * Num_Rings3 + 3.1125 * Num_Rings6 + 0.88274 * Num_RotatableBonds	0.9976	0.9937	0.8598	4.17E-06
7.	GFATempModel_7 = -3.0312–0.1573 * C_Count – 0.048019 * N_Count + 0.0026228 * Molecular_Mass + 0.95237 * Num_H_Donors – 2.7969 * Num_RingAssemblies + 2.6027 * Num_Rings3 + 3.0261 * Num_Rings6 + 0.84102 * Num_RotatableBonds	0.9975	0.9936	0.9237	4.40E-06
8.	GFATempModel_8 = -3.7494 + 0.14322 * O_Count – 0.0059193 * Molecular_Mass + 0.07357 * Num_AromaticBonds + 0.83293 * Num_H_Donors – 2.0552 * Num_RingAssemblies + 3.4906 * Num_Rings3 + 2.4363 * Num_Rings6 + 0.76509 * Num_RotatableBonds	0.9973	0.993	0.9751	5.36E-06
9.	GFATempModel_9 = -2.8723–0.11324 * C_Count + 0.078083 * O_Count – 0.066154 * HBA_Count + 0.85671 * Num_H_Donors – 2.424 * Num_RingAssemblies + 2.7191 * Num_Rings3 + 2.7878 * Num_Rings6 + 0.81744 * Num_RotatableBonds	0.997	0.9923	0.778	6.81E-06
10.	GFATempModel_10 = -3.2288–0.05648 * H_Count + 0.01213 * Num_BridgeBonds + 0.98205 * Num_H_Donors – 0.084766 * Num_H_Donors_Lipinski – 2.5418 * Num_RingAssemblies + 2.8971 * Num_Rings3 + 2.6477 * Num_Rings6 + 0.79772 * Num_RotatableBonds	0.997	0.9923	0.9578	6.82E-06

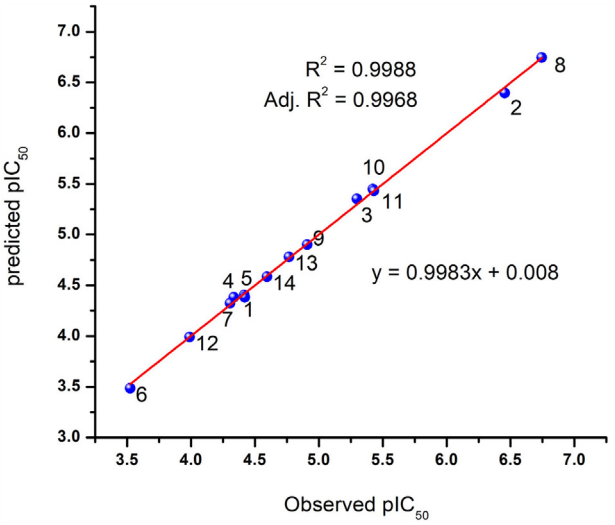

Fig. 4. Correlation between the actual and predicted activities of HK-2 cells from the recommended QSAR model.

(EC-GA) method was used to identify pharmacophore groups and bioactivity prediction based on electronic structure and conformational parameters [42,43]. However, 3D or 4D QSAR requires a relatively large and chemically diverse training set, and the predictive ability of QSAR was limited by the determination of quantum chemical calculation in three-dimensional space [44–46].

In other cases, the QSAR model with the predictive ability provides toxicological guidance on unknown hazardous substances [47]. However, the potential molecular descriptors of the nephrotoxic drugs are still under investigated. Therefore, we investigated fourteen marked drug and their nephrotoxicity to generate reasonable QSAR models for hazardous properties identification in this study. As for the result of QSAR modeling, we analyzed the descriptors suggested from the ten different generated equation models responsible for the toxic effects of HK-2 cell. According to the best reasonable linear regression model of HK-2 cells, the suggested molecular descriptors were **C_Count, Num_BridgeBonds, Num_H_Donors, Num_NegativeAtoms, Num_RingAssemblies, Num_Rings3, Num_Rings6,** and **Num_RotatableBonds.** We noted that descriptors such as Num_RingAssemblies, Num_Rings3, and Num_Rings6 with high value of the estimated regression coefficients among the best reasonable equation, and the value of the above three coefficients are – 2.7209, 2.7209, and 2.9782, respectively. Therefore, these three properties were regarded as critical features and be used to further study the difference among all tested compounds.

Comparing the numerical properties of the fourteen compounds, compound **1** had a similar quantitative value of suggested descriptors to compound **14**. These two compounds with similar numbers of **Num_RingAssemblies**, **Num_Rings3**, and **Num_Rings6**. However, the compound **1** have more inhibitory effects than compound **14** due to the difference in **C_Count**, **Num_H_Donors**, and **Num_RotatableBonds** descriptors. The compound **1** has less numbers of carbon atoms and H-bond donors than compound **14**. In contrast, compounds **1** have more numbers of rotatable bonds than compound **14**, suggesting that **Num_RotatableBonds** descriptors is favored property while **C_Count** and **Num_H_Donors** are disfavor properties to increase the toxic effects. In an earlier report, Yinping Shi et al. indicated that molecular weight, molecular polar surface area, AlogP, number of hydrogen bond acceptors, molecular solubility, the number of rotatable bonds, and the number of aromatic rings were critical physical–chemical properties in the identification of nephrotoxic drugs [48]. In comparison with the aforementioned properties, our suggested equation of the QSAR model had identical or similar features such as rotatable bonds, organic rings, and hydrogen bonds. In addition, Yinping Shi et al.'s study demonstrated that chemical hydrogen

Table 3
The predicted data from the recommended equation of QSAR model.

Comp.	Bioactivity (μM)	Actual value (pIC_{50})	Predicted value (pIC_{50})	Residual error
1	0.18	6.74	6.75	0
2	12.31	4.91	4.9	0.01
3	46.15	4.34	4.38	−0.05
4	37.86	4.42	4.38	0.04
5	0.35	6.46	6.4	0.06
6	3.77	5.42	5.45	−0.03
7	102.6	3.99	3.99	0
8	17.14	4.77	4.78	−0.02
9	49.39	4.31	4.33	−0.02
10	5.04	5.3	5.35	−0.06
11	299.6	3.52	3.49	0.04
12	25.45	4.59	4.59	0.01
13	3.7	5.43	5.43	0
14	38.27	4.42	4.41	0.01

Table 4
The quantitative values of the chemical descriptors from the recommended equation of QSAR model.

Comp.	Activity		Molecular property							
	IC_{50} (μM)	pIC_{50}	C_Count	Num_BridgeBonds	Num_H_Donors	Num_NegativeAtoms	Num_RingAssemblies	Num_Rings3	Num_Rings6	Num_RotatableBonds
1	0.18	6.74	34	0	2	0	1	0	0	17
5	0.35	6.46	17	9	3	0	1	1	2	3
13	3.7	5.43	47	40	11	1	2	0	2	3
6	3.77	5.42	17	9	2	0	1	1	2	3
10	5.04	5.3	15	0	4	0	1	1	1	4
2	12.31	4.91	15	9	3	0	1	1	2	1
8	17.14	4.77	22	0	1	0	2	0	3	7
12	25.45	4.59	0	0	2	2	1	3	0	0
4	37.86	4.42	20	0	2	1	2	0	3	5
14	38.27	4.42	62	0	5	0	1	0	0	15
3	46.15	4.34	20	0	2	1	2	0	3	5
9	49.39	4.31	44	25	3	0	2	0	3	7
7	102.6	3.99	17	0	0	2	1	0	3	3
11	299.6	3.52	16	0	2	0	2	0	2	7

bonding ability is an important feature responsible for toxicity and bioactivity. Meanwhile, their data indicated that the number of hydrogen bond acceptors was obviously related to nephrotoxicity but the number of hydrogen bond donors was not. Interestingly, the number of hydrogen bond donors was also considered a disfavor property based on the analyzed results. Therefore, our suggested molecular properties might have responsible for nephrotoxic structures.

Note that compounds **9**, **11**, and **13** each have similar values of **Num_RingAssemblies**, **Num_Rings3**, and **Num_Rings6** descriptors. For the less toxic effects of compounds **9** and **11**, the compound **13** has more numbers of carbon atoms, H-bond donors, and bonds in bridgehead ring systems than compound **11**. Interestingly, the compound **13** has one **Num_NegativeAtoms** descript than compounds **9** and **11**, indicating that the negative atom might be the critical property increased significantly the toxic effect for HK-2 cells.

Among our tested drugs, the compounds **2, 5** and **6** have similar moiety on chemical structure. Regarding the compounds with more numbers of **C_Count**, **Num_H_Donors**, and **Num_RotatableBonds** descriptors, compound **5** had more toxic effects on HK-2 cells than compounds **2** and **6**. The compound **5** and **6** have seventeen carbon atoms and three rotatable bonds, while compounds **2** has fifteen carbon atoms and one rotatable bond. The finding indicated that a greater number of carbon atoms and rotatable bonds may increase the toxic effect on renal cells.

It should be emphasized that we report the first attempt to link the experimentally revealed toxic effects of marked drugs to the peculiarities of their molecular properties based on QSAR analysis. The QSAR model developed in this study provide very useful information on relationships between the chemical structure of the marked drugs and their toxic effects, which can help to analyze the nephrotoxicity for more therapeutic drug.

5. Conclusion

To assess kidney toxicity, the equations of QSAR modeling were generated based on fourteen therapeutic drugs and their inhibitory effects discovered critical structural features on the renal cells. The aim of this study is not only employing the in vitro cell-based studies, but also include the in silico methods as supporting tools that used for identification of the potential toxicity from chemical properties. According to the suggested equation of QSAR models, the most toxic compound **1** with more numbers of rotatable bonds had stronger toxicity effects on HK-2 cells. In addition, increase in the number of bridge bond, H-bond donors, and negative atoms in the structures of the test compounds could promote the toxic effect. The current study demonstrated that the current used drug with no common structure can be observe a tendency on nephrotoxic effect based on QSAR modeling, which may help to provide useful information on discovery of hazardous property for renal preventive medicine in the future.

CRediT authorship contribution statement

Hung-Jin Huang: Conceptualization, Methodology, Data curation, Writing – review & editing. **Yu-Hsuan Lee:** Conceptualization, Methodology. **Chu-Lin Chou:** Conceptualization, Methodology. **Cai-Mei Zheng:** Conceptualization, Writing – review & editing,

Supervision. **Hui-Wen Chiu:** Conceptualization, Writing – review & editing, Supervision.

Declaration of Competing Interest

The authors declare that they have no known competing financial interests or personal relationships that could have appeared to influence the work reported in this paper.

Acknowledgments

This study was supported by the Ministry of Science and Technology, Taiwan (MOST 108-2314-B-039-061-MY3, MOST 109-2314-B-038-078-MY3, MOST 110-2314-B-038-140 and MOST 110-2314-B-038-075-MY3) and China Medical University, Taichung, Taiwan (CMU110-N-20).

Appendix A. Supplementary data

Supplementary data to this article can be found online at https://doi.org/10.1016/j.csbj.2022.04.013.

References

[1] Wang X, Yang S, Li S, Zhao L, Hao Y, et al. Aberrant gut microbiota alters host metabolome and impacts renal failure in humans and rodents. Gut 2020;69(12):2131.
[2] Al-Kuraishy HM, Al-Gareeb A, Hussien NR. Betterment of diclofenac-induced nephrotoxicity by pentoxifylline through modulation of inflammatory biomarkers. Asian J Pharm Clin Res 2019;12(3):433–7.
[3] Zhao Y-Y, Lin R-C, Chapter Three - Metabolomics in Nephrotoxicity, in: G.S. Makowski (Ed.) Adv Clin Chem, Elsevier2014, pp. 69-89.
[4] Sri Laasya TP, Thakur S, Poduri R, Joshi G. Current insights toward kidney injury: Decrypting the dual role and mechanism involved of herbal drugs in inducing kidney injury and its treatment. Curr Opin Biotechnol 2020;2:161–75.
[5] Uber AM, Sutherland SM. Nephrotoxins and nephrotoxic acute kidney injury. Pediatr Nephrol 2020;35(10):1825–33.
[6] Georgianos PI, Agarwal R. Hypertension in chronic kidney disease (CKD): Diagnosis, classification, and therapeutic targets. Am J Hypertens 2020;34(4):318–26.
[7] Lim YJ, Sidor NA, Tonial NC, Che A, Urquhart BL. Uremic Toxins in the Progression of Chronic Kidney Disease and Cardiovascular Disease: Mechanisms and Therapeutic Targets. Toxins 2021;13(2).
[8] Kellum JA, Romagnani P, Ashuntantang G, Ronco C, Zarbock A, et al. Acute kidney injury. Nat Rev Dis Primers 2021;7(1):52.
[9] Rolland A-L, Garnier A-S, Meunier K, Drablier G, Briet M. Drug-Induced Acute Kidney Injury: A Study from the French Medical Administrative and the French National Pharmacovigilance Databases Using Capture-Recapture Method. J Clin Med 2021;10(2).
[10] Patel JB, Sapra A. Nephrotoxic Medications, StatPearls, StatPearls Publishing Copyright © 2022. FL: StatPearls Publishing LLC., Treasure Island; 2022.
[11] Okoro RN, Farate VT. The use of nephrotoxic drugs in patients with chronic kidney disease. Int J Clin Pharm 2019;41(3):767–75.
[12] Verzicco I, Regolisti G, Quaini F, Bocchi P, Brusasco I, et al., Electrolyte Disorders Induced by Antineoplastic Drugs, Front Oncol 2020;10.
[13] Petejova N, Martinek A, Zadrazil J, Kanova M, Klementa V, et al. Acute kidney injury in septic patients treated by selected nephrotoxic antibiotic agents—pathophysiology and biomarkers—A review. Int J Mol Sci 2020;21(19).
[14] Perazella MA. Drug-induced acute kidney injury: diverse mechanisms of tubular injury. Curr Opin Crit Care 2019;25(6).
[15] Liu C, Yan S, Wang Y, Wang J, Fu X, et al. Drug-Induced hospital-acquired acute kidney injury in China: A multicenter cross-sectional survey. Kidney Dis-Basel 2021;7(2):143–55.
[16] Awdishu L, Mehta RL. The 6R's of drug induced nephrotoxicity. BMC Nephrol 2017;18(1):124.
[17] Hoste EAJ, Bagshaw SM, Bellomo R, Cely CM, Colman R, et al. Epidemiology of acute kidney injury in critically ill patients: the multinational AKI-EPI study. Intensive Care Med 2015;41(8):1411–23.
[18] Huang H-J, Lee Y-H, Hsu Y-H, Liao C-T, Lin Y-F, et al. Current strategies in assessment of nanotoxicity: alternatives to in vivo animal testing. Int J Mol Sci 2021;22(8).
[19] Alves VM, Auerbach SS, Kleinstreuer N, Rooney JP, Muratov EN, et al. Curated data in — trustworthy in silico models out: the impact of data quality on the reliability of artificial intelligence models as alternatives to animal testing. Altern Lab Anim 2021;49(3):73–82.
[20] Zheng Z, Arp HPH, Peters G, Andersson PL. Combining in silico tools with multicriteria analysis for alternatives assessment of hazardous chemicals: accounting for the transformation products of decaBDE and its alternatives. Environ Sci Technol 2021;55(2):1088–98.
[21] Kuhlmann C, Schenck TL, Tluczynski K, Aszodi A, Metzger P, et al. Experimental approach to nasal septal cartilage regeneration with adipose tissue-derived stem cells and decellularized porcine septal cartilage. Xenotransplantation 2021;28(2):e12660.
[22] Falk MJ. The pursuit of precision mitochondrial medicine: Harnessing preclinical cellular and animal models to optimize mitochondrial disease therapeutic discovery. J Inherit Metab Dis 2021;44(2):312–24.
[23] Cadena M, Ning L, King A, Hwang B, Jin L, et al. 3D Bioprinting of neural tissues. Adv Healthc Mater 2021;10(15):2001600.
[24] Leoni C, Gattulli BAR, Pesole G, Ceci LR, Volpicella M. Amylomaltases in extremophilic microorganisms. Biomolecules 2021;11(9).
[25] Rim K-T. In silico prediction of toxicity and its applications for chemicals at work. Toxicol Environ Health Sci 2020;12(3):191–202.
[26] Benfenati E, Chaudhry Q, Gini G, Dorne JL. Integrating in silico models and read-across methods for predicting toxicity of chemicals: A step-wise strategy. Environ Int 2019;131:105060.
[27] Kosugi Y, Hosea N. Prediction of oral pharmacokinetics using a combination of in silico descriptors and in vitro ADME properties. Mol Pharm 2021;18(3):1071–9.
[28] Wang D, Rietdijk MH, Kamelia L, Boogaard PJ, Rietjens IMCM. Predicting the in vivo developmental toxicity of benzo[a]pyrene (BaP) in rats by an in vitro–in silico approach. Arch Toxicol 2021;95(10):3323–40.
[29] Gupta R, Srivastava D, Sahu M, Tiwari S, Ambasta RK, et al. Artificial intelligence to deep learning: machine intelligence approach for drug discovery. Mol Divers 2021;25(3):1315–60.
[30] Mao J, Akhtar J, Zhang X, Sun L, Guan S, et al. Comprehensive strategies of machine-learning-based quantitative structure-activity relationship models. iScience 2021;24(9):103052.
[31] Huang H-J, Chetyrkina M, Wong C-W, Kraevaya OA, Zhilenkov AV, et al. Identification of potential descriptors of water-soluble fullerene derivatives responsible for antitumor effects on lung cancer cells via QSAR analysis. Comput Struct Biotechnol J 2021;19:812–25.
[32] Huang T, Sun G, Zhao L, Zhang N, Zhong R, et al. Quantitative structure-activity relationship (QSAR) studies on the toxic effects of nitroaromatic compounds (NACs): A systematic review. Int J Mol Sci 2021;22(16).
[33] Gu L, Lu J, Li Q, Huang W, Wu N, et al. Synthesis, extracorporeal nephrotoxicity, and 3D-QSAR of andrographolide derivatives. Chem Biol Drug Des 2021;97(3):592–606.
[34] Lee S, Kang Y-M, Park H, Dong M-S, Shin J-M, et al. Human nephrotoxicity prediction models for three types of kidney injury based on data sets of pharmacological compounds and their metabolites. Chem Res Toxicol 2013;26(11):1652–9.
[35] Mathioudakis NN, Abusamaan MS, Shakarchi AF, Sokolinsky S, Fayzullin S, et al. Development and validation of a machine learning model to predict near-term risk of iatrogenic hypoglycemia in hospitalized patients. JAMA Network Open 2021;4(1). e2030913-e2030913.
[36] Gholamy A, Kreinovich V, Kosheleva O, Why 70/30 or 80/20 relation between training and testing sets: A pedagogical explanation, 2018.
[37] Devolder K, Yip LJ, Douglas T. The Ethics of creating and using human-animal chimeras. ILAR J 2019;60(3):434–8.
[38] Huang H-J, Kraevaya OA, Voronov II, Troshin PA, Hsu S-H. Fullerene derivatives as lung cancer cell inhibitors: investigation of potential descriptors using QSAR approaches. Int J Nanomedicine 2020;15:2485–99.
[39] Gajewicz-Skretna A, Furuhama A, Yamamoto H, Suzuki N. Generating accurate in silico predictions of acute aquatic toxicity for a range of organic chemicals: Towards similarity-based machine learning methods. Chemosphere 2021;280:130681.
[40] Durdagi S, Erol I, Salmas RE, Patterson M, Noskov SY. First universal pharmacophore model for hERG1 K+ channel activators: acthER. J Mol Graph Model 2017;74:153–70.
[41] Salmas RE, Stein M, Yurtsever M, Seeman P, Erol I, et al. The signaling pathway of dopamine D2 receptor (D2R) activation using normal mode analysis (NMA) and the construction of pharmacophore models for D2R ligands. J Biomol Struct Dyn 2017;35(9):2040–8.
[42] Sahin K, Saripinar E, Durdagi S. Combined 4D-QSAR and target-based approaches for the determination of bioactive Isatin derivatives. SAR QSAR Environ Res 2021;32(10):769–92.
[43] Sahin K, Saripinar E. A novel hybrid method named electron conformational genetic algorithm as a 4D QSAR investigation to calculate the biological activity of the tetrahydrodibenzazosines. J Comput Chem 2020;41(11):1091–104.
[44] Cherkasov A, Muratov EN, Fourches D, Varnek A, Baskin II, et al. QSAR Modeling: Where Have You Been? Where Are You Going To? J Med Chem 2014;57(12):4977–5010.
[45] Jagiello K, Grzonkowska M, Swirog M, Ahmed L, Rasulev B, et al. Advantages and limitations of classic and 3D QSAR approaches in nano-QSAR studies based on biological activity of fullerene derivatives. J Nanopart Res 2016;18(9):256.
[46] Andrade CH, Pasqualoto KFM, Ferreira EI, Hopfinger AJ. 4D-QSAR: perspectives in drug design. Molecules 2010;15(5).
[47] Chinen K, Malloy T. QSAR Use in REACH analyses of alternatives to predict human health and environmental toxicity of alternative chemical substances. Integr Environ Assess Manag 2020;16(5):745–60.
[48] Shi Y, Hua Y, Wang B, Zhang R, Li X. In silico Prediction and insights into the structural basis of drug induced nephrotoxicity. Front Pharmacol 2022;12.